JAERI - M
88-023

# NUMERICAL CALCULATION OF HIGH FREQENCY FAST WAVE CURRENT DRIVE IN A REACTOR GRADE TOKAMAK

February 1988

Kenkichi USHIGUSA and Kiyotaka HAMAMATSU

日 本 原 子 力 研 究 所
Japan Atomic Energy Research Institute

JAERI-Mレポートは，日本原子力研究所が不定期に公刊している研究報告書です。
入手の問合わせは，日本原子力研究所技術情報部情報資料課（〒319-11茨城県那珂郡東海村）あて，お申しこしください。なお，このほかに財団法人原子力弘済会資料センター（〒319-11 茨城県那珂郡東海村日本原子力研究所内）で複写による実費頒布をおこなっております。

JAERI-M reports are issued irregularly.
Inquiries about availability of the reports should be addressed to Information Division, Department of Technical Information, Japan Atomic Energy Research Institute, Tokai-mura, Naka-gun, Ibaraki-ken 319-11, Japan.



編集兼発行　日本原子力研究所
印　　刷　㈱原子力資料サービス

JAERI-M 88-023

# Numerical Calculation of High Frequency Fast Wave Current Drive in a Reactor Grade Tokamak

Kenkichi USHIGUSA and Kiyotaka HAMAMATSU

Department of Large Tokamak Research
Japan Atomic Energy Research Institute
Naka Fusion Research Establishment
Naka-machi, Naka-gun, Ibaraki-ken

(Received January 27, 1988)

A fast wave current drive with a high frequency is estimated for a reactor grade tokamak by the ray tracing and the quasi-linear Fokker-Planck calculations with an assumption of single path absorption. The fast wave can drive RF current with the drive efficiency of $\eta_{CD} = \bar{n}_e(10^{19}\ m^{-3})I_{RC}(A)R(m)/P_{RF}(W) \sim 3.0$ when the wave frequency is selected to be $f/f_{ci} > 7$. A sharp wave spectrum and a $<v_{ph\parallel}>/v_{Te} \sim 3.0$ are required to obtain a good efficiency. A center peaked RF current profile can be formed with an appropriate wave spectrum even in the high temperature plasma.

Keywords: Fast Wave, High Frequency, Current Drive, Tokamak Reactor

# トカマク炉における高周波速波電流駆動の数値計算

日本原子力研究所那珂研究所臨界プラズマ研究部
牛草　健吉・濱松　清隆

（1988年1月27日受理）

炉心プラズマパラメータを持つトカマクプラズマでの高い周波数を持つ速波による電流駆動を評価した。評価法は，レイ軌跡計算と準線形フォッカープランクコードを用い，シングルパル吸収を仮定した。周波数が $f / f_{ci} > 7$ の速波は，電流駆動効率 $\eta_{CD} \equiv \bar{n}_e(10^{19}m^{-3})\, I_{RF}(A)\, R_P(m) / R_{RF}(W) \sim 3.0$ で電流を駆動できる。鋭い分布のスペクトルを持ち，電子熱速度の3倍程度の位相速度の波を励起すると良い駆動効率が得られる。高い電子温度のプラズマにおいても，適当な放射スペクトルを持った速波を入射することにより，中心にピークするＲＦ電流分布を得ることができる。

那珂研究所：〒311－01　茨城県那珂郡那珂町大字向山801－1

Contents



# 目　　次

## 1. Introduction

The RF current drive is one of the most promising method to realize the steady state tokamak reactor. Recent experiments in JT-60[1] show that 2MA of the plasma current has been sustained by the lower hybrid wave and the current drive efficiency has been improved to $\eta_{CD} = \bar{n}_e(10^{19}\mathrm{m}^{-3})R(\mathrm{m})I_{RF}(\mathrm{A})/P_{RF}(\mathrm{W})$=1.5-3.0 from 0.8-1.5 by the combination of the lower hybrid current drive(LHCD) and the neutral beam heating in relatively low density plasma. Furthermore results of the combined neutral beam heating with the LHCD plasma show RF current drive can improve the energy confinement time in the beam heated plasma[12]. It has been suggested that the flattening of the current profile by the RF current drive is a key factor to obtain the improvement of energy confinement. As shown in these results the RF current drive is quite attractive to employ the next generation tokamak for the steady state operation and the control the confinement property.

In the high density and the high temperature plasma such as the reactor grade tokamak the LHCD has some difficult problems. The first problem is the density limit of LHCD which is supposed to be caused by parametric instabilities[3]. In order to avoid parametric instabilities, a higher wave frequency may be required. At the same time the high toroidal magnetic field is required because the accessibility condition becomes a severe problem in such a high frequency LHCD[4]. The second problem is the controllability of the current profile. The LHW may cause a surface current in a high temperature reactor grade discharge because the electron damping rate may be quite high in a high temperature peripheral plasma[5]. The fast wave current drive(FWCD) which has a high frequency may remove such problems. It is supposed that the fast wave does not have the density limit of the interaction between the wave and the electron such as the lower hybrid wave when an appropriate wave frequency is

selected[6]. The fast wave which has a low $n_{\parallel}$ can penetrate to the high density plasma. Furthermore the fast wave has a smaller wave electric field along the magnetic field than that of the lower hybrid wave. This means that the RF current profile of FWCD does not tend to be a surface current in the high temperature plasma such as a reactor grade tokamak.

In order to confirm these merits of FWCD in the reactor grade plasma the numerical estimation of FWCD is examined in this paper. The numerical model is described in next section. Numerical results are shown in section 2 and section 3 summarizes this study. Finally, FWCD is estimated for the JT-60 parameters in Appendix.

## 2. Numerical model

The employed model consists of a ray tracing code and a Fokker-Planck code. This model estimates the absorption power and the RF current in the single ray path. The ray tracing code calculates the wave propagation and the power deposition to the ion by the ion cyclotron harmonic damping. The RF current and the wave damping through the electron absorption are calculated by the quasi-linear Fokker-Planck calculation using results of the ray tracing code.

### 2.1 Ray tracing code

A dispersion relation of the cold plasma is employed for the calculation of ray trajectories. This assumption is supported by one dimensional kinetic code[7]. The dispersion relation of the cold plasma is described by

$$G = A\,k_{\perp}^4 + B\,k_{\perp}^2 + C = 0, \qquad (2\text{-}1)$$

selected[6]. The fast wave which has a low $n_{\parallel}$ can penetrate to the high density plasma. Furthermore the fast wave has a smaller wave electric field along the magnetic field than that of the lower hybrid wave. This means that the RF current profile of FWCD does not tend to be a surface current in the high temperature plasma such as a reactor grade tokamak.

In order to confirm these merits of FWCD in the reactor grade plasma the numerical estimation of FWCD is examined in this paper. The numerical model is described in next section. Numerical results are shown in section 2 and section 3 summarizes this study. Finally, FWCD is estimated for the JT-60 parameters in Appendix.

## 2. Numerical model

The employed model consists of a ray tracing code and a Fokker-Planck code. This model estimates the absorption power and the RF current in the single ray path. The ray tracing code calculates the wave propagation and the power deposition to the ion by the ion cyclotron harmonic damping. The RF current and the wave damping through the electron absorption are calculated by the quasi-linear Fokker-Planck calculation using results of the ray tracing code.

### 2.1 Ray tracing code

A dispersion relation of the cold plasma is employed for the calculation of ray trajectories. This assumption is supported by one dimensional kinetic code[7]. The dispersion relation of the cold plasma is described by

$$G = A\,k_{\perp}^4 + B\,k_{\perp}^2 + C = 0, \qquad (2\text{-}1)$$

where

$$A = (c/\omega)^4 S$$

$$B = (c/\omega)^2(-(S+P)(S-n_{\parallel}^2)+D^2)$$

$$C = P((S-n_{\parallel}^2)^2 - D^2)$$

$$S = 1 + \frac{\omega_{pe}^2}{\omega_{ce}^2} - \frac{\omega_{pi}^2}{\omega^2 - \omega_{ci}^2} \qquad (2\text{-}2)$$

$$D = \frac{\omega_{pe}^2}{\omega\omega_{ce}} + \frac{\omega_{pi}^2\omega_{ci}}{\omega(\omega^2 - \omega_{ci}^2)}$$

$$P = 1 - \frac{\omega_{pe}^2}{\omega^2} - \frac{\omega_{pi}^2}{\omega^2}$$

and $\omega_{pe}/2\pi$, $\omega_{pi}/2\pi$, $\omega_{ce}/2\pi$, $\omega_{ci}/2\pi$ and $\omega/2\pi$ are the electron,the ion plasma frequency, the electron, the ion cyclotron frequency and the wave frequency, respectively. The refractive index along the magnetic field $n_{\parallel}$, the parallel and the perpendicular wave number $k_{\parallel}$,$k_{\perp}$ are described as

$$n_{\parallel} = \frac{c\,k_{\parallel}}{\omega}$$

$$k_{\parallel} = \frac{m}{r}\sin\beta + \frac{n}{R}\cos\beta \qquad (2\text{-}3)$$

$$k_{\perp}^2 = k_r^2 + \left(\frac{m}{r}\cos\beta - \frac{n}{R}\sin\beta\right)^2,$$

where $R = R_o + r\cos\theta$,$\beta = \tan^{-1}(B_\theta/B_\varphi)$, $k_r$, $n$ , $m$ are the radial wave number, the poloidal and the toroidal mode number. $B_\theta$ and $B_\varphi$ are the poloidal and the toroidal magnetic field.

Ray trajectories are calculated by solving the following ray equations.

$$\frac{dr}{dt} = -\frac{\frac{\partial G}{\partial k_r}}{\frac{\partial G}{\partial \omega}}$$

$$\frac{d\theta}{dt} = -\frac{\frac{\partial G}{\partial m}}{\frac{\partial G}{\partial \omega}}$$

$$\frac{dk_r}{dt} = \frac{\frac{\partial G}{\partial r}}{\frac{\partial G}{\partial \omega}} \qquad (2\text{-}4)$$

$$\frac{dm}{dt} = \frac{\frac{\partial G}{\partial \theta}}{\frac{\partial G}{\partial \omega}}$$

From a symmetry of the toroidal direction the toroidal mode number n is conserved. As the initial condition, the wave number is set so that the dispersion of the fast wave is satisfied. The calculation of ray path is ended when the ray reaches the minimal radius.

In order to estimate the power deposition to the ion the linear ion cyclotron harmonic damping is assumed. The damping rate is described by

$$\gamma_i = -\frac{\frac{\partial G}{\partial S}}{\frac{\partial G}{\partial \omega}} \mathrm{Im}(S)$$

$$\mathrm{Im}(S) = \sum_{l=1}^{\infty} l^2 \frac{\omega_{pi}^2}{\omega^2} \sqrt{\pi}\, \chi_i \frac{e^{-(\lambda_i)}}{\lambda_i} I_l(\lambda_i) \exp\left[ -\chi_i^2 (1 - l^2 \frac{\omega_{ci}^2}{\omega^2}) \right] \qquad (2\text{-}5)$$

where

$$\chi_i = \frac{\omega}{k_{\parallel} v_{Ti}}$$

$$v_{Ti} = \frac{2\,T_i}{m_i} \qquad (2\text{-}6)$$

$$\lambda_i = \frac{k_i^2 v_{Ti}^2}{2\,\omega_{ci}^2}$$

and $I_l(\lambda_i)$ is the modified Bessel function of $l$th order.

### 2.2 Quasi-linear Fokker-Planck calculation

The RF current and the power absorption to the electron are calculated by one-dimensional quasi-linear Fokker-Planck equation[7]

$$\frac{\partial}{\partial v_{\parallel}}\left[ (D_{ql}+D_c)\frac{\partial F}{\partial v_{\parallel}} + \nu(v_{\parallel})\, v_{\parallel} F \right] = 0 \tag{2-7}$$

where

$$D_{ql} = \pi \frac{e}{m_e}^2 \frac{\hat{E}_z^2(k_{\parallel})}{v_{\parallel}}\bigg|_{k_{\parallel}=\frac{\omega}{v_{\parallel}}}$$

$$D_c = v_e^2 \nu(v_{\parallel})$$

$$\nu(v_{\parallel}) = \nu_0 g(\frac{v_{\parallel}}{v_e})$$

$$g(u) = \frac{Z_{eff}}{4\sqrt{2}} G(\frac{u^2}{2}) + \frac{1}{3\sqrt{2\pi}+|u|^3} \tag{2-8}$$

$$G(x) = \sqrt{\pi}\exp(x)\left[1+\Phi(\sqrt{x})\right](1+2x) - 2\sqrt{x}$$

$$\nu_0 = \frac{\omega_{pe}^4 \ln\Lambda}{2\pi n_e v_e^3}$$

and $v_e^2 = T_e/m_e$, $\Phi(x)$ is the error function, $E_z(k_{\parallel})$ and $\ln\Lambda$ are the wave electric field along the magnetic field and the Coulomb logarithm. The electron velocity distribution function $F$, the RF current $j_{RF}$ and the absorption power of electrons $p_{abs}^e$ are described as following equations

$$F(v_\parallel) = C\ \exp\left(\int_{-\infty}^{v_\parallel} \frac{u\,du}{1+\hat{D}_w}\right)$$

$$j_{RF} = e n_e v_e \int_{-\infty}^{\infty} u F\,du \tag{2-9}$$

$$p^e_{abs} = m_e n_e v_e^2 \nu_0 \int_{-\infty}^{\infty} g(u) u^2 \frac{\hat{D}_w}{1+\hat{D}_w} F\,du$$

where $u = v_\parallel / v_e, C = 1/\int_{-\infty}^{\infty} F\,du$, and $\hat{D}_w = D_w / D_c$.

The RF electric field along the magnetic field $E_\parallel(v_\parallel)$ is calculated from the magnetic surface averaged wave energy density $W_o$

$$W_o = \frac{P(n_{\parallel i})}{|v_{gr(n_{\parallel i})}| 2\pi R_o 2\pi r} \tag{2-10}$$

with a correction of TTMP term described as

$$\hat{E}_\parallel^2 = E_\parallel^2 (1 - k_\perp^2 \rho_e^2) + 2\frac{k_\parallel k_\perp \rho_e v_e}{\omega}\left\{\mathrm{Im}(E_\parallel^* E_y) + \frac{k_\parallel k_\perp \rho_e v_e}{\omega} E_y^2\right\} \tag{2-11}$$

where

$$W_o = \frac{1}{2}\left[\frac{\vec{B}^* \cdot \vec{B}}{2\mu_o} + \frac{\varepsilon_o}{2}\vec{E}^* \cdot \frac{\partial K}{\partial \omega} \cdot \vec{E}\right]$$

$$\vec{B} = \vec{k} \times \vec{E} \tag{2-12}$$

and $K$ is the dielectric tensor of the cold plasma, $P(n_{\parallel i})$ is the wave power having the parallel refractive index of $n_{\parallel i}$, $v_{gr}(n_{\parallel i})$ is the radial group velocity, and $\rho_e$ is the larmor radius of the electron.

## 2.3 Parameter profiles

Profiles of the electron density $n_e(r)$, the electron temperature $T_e(r)$, the ion temperature $T_i(r)$, the radial, the poloidal and the toroidal magnetic field $B_r(r)$,$B_\theta(r)$ and $B_\varphi(r)$ are assumed as

$$
\begin{aligned}
n_e(r) &= n_e(0)\left[(1-(\frac{r}{a})^2)^{\alpha_{ne}} + C_{ne}\right] \\
T_e(r) &= T_e(0)\left[(1-(\frac{r}{a})^2)^{\alpha_{Te}} + C_{Te}\right] \\
T_i(r) &= T_i(0)\left[(1-(\frac{r}{a})^2)^{\alpha_{Ti}} + C_{Ti}\right] \\
B_r(r) &= 0 \\
B_\theta(r) &= \frac{\mu_o I_p}{\pi r}(1-\frac{r^2}{2a^2})\frac{r^2}{a^2} \\
B_\varphi &= \frac{B_\varphi(0)}{1+\frac{r}{R_o}\cos\theta}
\end{aligned}
\qquad (2\text{-}13)
$$

The radiated wave power spectrum from the launcher is assumed to be Gaussian profile as

$$
S(n_\parallel) = \exp\left[-\left\{\frac{n_\parallel - n_\parallel(0)}{\Delta n_\parallel/2}\right\}^2\right] - \text{Const.} \qquad (2\text{-}14)
$$

where $n_\parallel(0)$,$\Delta n_\parallel$ are the center value of $n_\parallel$, the width of the spectrum. The power spectrum is divided into typically fifty elements and for each element the wave trajectory is calculated.

## 3. Numerical results

The fast wave current drive in the parameters of the reactor grade tokamak is estimated in this section. Typical plasma parameters in this case are summarized in Table 1.

Figure 1 shows frequency dependences of the current drive efficiencies $\eta_e$,$\eta_T$ and the single path absorption rate $\eta_{abs}$, where $\eta_e = I_{RF}/P_e$,$\eta_T = I_{RF}/(P_e+P_i)$ and $P_e$,$P_i$,$P_{in}$ are the absorption power to electrons, ions, the input power. Typical plasma parameters except with the frequency are in Table 1. At the low frequency regime the ion damping cannot be ignored so that the total drive efficiency $\eta_T$ is low. When the frequency f is larger than 0.3GHz, this frequency corresponds to $f/f_{ci}>7$, the ion damping becomes small. Efficiencies $\eta_e$ and $\eta_T$ increase with the frequency $f$, while the single path absorption rate $\eta_{abs} = (P_e+P_i)/P_{in}$ becomes small. This is caused by the change of $n_\parallel$ with the wave propagation. At a higher frequency, the parallel refractive index $n_\parallel$ tends to decrease and the wave phase velocity $v_{ph\parallel}$ increases. The ratio of $v_{ph\parallel}$ to the thermal velocity shifts to larger region where the $\eta_{CD}$ is high[8].

The current drive efficiency $\eta_e=I_{RF}/P_e$ and $P_e/P_{in}$ are plotted in Fig. 2 as a function of the central electron temperature $T_e(0)$ where $n_\parallel = 1\sim2$ and $f$=0.4GHz. The efficiency $\eta_e$ increases almost linearly with $T_e(0)$. At $T_e(0) = 40$keV, 60% of the input power is absorbed by electrons and $\eta_e = 0.08$A/W can be expected. This value corresponds to the usually normalized current drive efficiency $\eta_{CD} = \bar{n}_e(10^{19}\mathrm{m}^{-3})R(\mathrm{m})I_{RF}(\mathrm{A})/P_{RF}(\mathrm{W})\sim3.0$. Fast wave may drive the RF current with enough efficiency, and the estimated efficiency is comparable to that of the lower hybrid wave.

The density dependence of the efficiency $\eta_T$, $P_{abs}=P_e+P_i$ and $\bar{n}_e I_{RF}/P_{abs}$ are shown in Fig.3 where $f$=0.4GHz, $T_e(0)=T_i(0)=30$keV. The efficiency $\eta_T$ is roughly proportional to $1/\bar{n}_e$ and so $\bar{n}_e I_{RF}/P_{abs}$ is almost constant.

Figure 4 shows the efficiency $\eta_T$ and the single path absorption rate

$\eta_{abs}$ as a function of the width of wave phase velocity normalized the mean phase velocity where $n_{\parallel}(0)$=1.5, $f$=0.4GHz, $T_e(0)$=30keV and $\bar{n}_e$= 7x10$^{19}$m$^{-3}$. The sharp spectrum leads to a good current drive efficiency. The low phase velocity component in the wave spectrum damps and drives the current in the relatively low temperature region where the collisional dissipation is large.

Figure 5 shows the mean phase velocity dependence of the $\eta_e$ and $\eta_{abs}$ for the wide spectrum case ($\Delta n_{\parallel}$=1.0) and for the narrow case ($\Delta n_{\parallel}$=0.2) where $<v_{ph\parallel}> = c/\, n_{\parallel(0)}$. The efficiency $\eta_T$ increases with the phase velocity while the single absorption rate decreases. When $<v_{ph\parallel}>/v_{Te}$ > 3.0 the electron absorption power is so small that the ion damping cannot be negligible. Therefore the total current drive efficiency is decreases in such region. It should be noted that if the ion damping is neglected the efficiency increases with $<v_{ph\parallel}>/v_{Te}$[8]. There is no large difference on $\eta_T$ and $\eta_{abs}$ in the low phase velocity between the wide spectrum case and the narrow case, while in the high phase velocity the efficiency $\eta_T$ of the wide spectrum is lower than that of the narrow one as mentioned before.

The RF current profiles for various $n_{\parallel}(0)$ are shown in Fig. 6 where $\Delta n_{\parallel}$=1.0 and the input power is adjusted so that the RF current becomes 8MA. The RF current profile tends to be broad when the launched spectrum has a large $n_{\parallel}(0)$. In the case of the fast wave current drive, the center-peaked current profile can be expected even in the reactor grade high electron temperature as shown in this figure ( in this case $T_e(0)$=30keV). The parallel electric field of the fast wave is smaller than that of the lower hybrid wave. This leads that the fast wave current drive does not tend to form the surface current as compared with LHCD. Figure 6 shows that the fast wave current drive has the capability to control the plasma current profile even in the reactor grade high temperature plasma.

## 4. Summary

The FWCD is examined for a reactor grade tokamak plasma by using the ray tracing code and the quasi-linear Fokker-Planck code. When the wave frequency is selected to $f/f_{ci}>7$ with an appropriate wave spectrum, the ion cyclotron damping can be neglected and the normalized current drive efficiency $\eta_{CD}=\bar{n}_e(10^{19}\mathrm{m}^{-3})I_{RF}(\mathrm{A})R(\mathrm{m})/P_{RF}(\mathrm{W})\sim 3.0$ can be expected in a high density ($\bar{n}_e=7\times10^{19}\mathrm{m}^{-3}$) and high temperature ($T_e$=40keV) plasma. The FWCD has the capability to control the current profile even in the reactor grade high temperature plasma.

The electron damping rate for the fast wave is weak even in high temperature plasma, for example, $P_{abs}/P_{in}\sim 0.6$ at $T_e$=40keV. The RF power which is not absorbed in single path propagation also contribute to drive RF current. We have to introduce the multiple-path effect[9] in order to more precise efficiency and RF current profile.

## Acknowledgements

The authors are grateful to Drs. T.Yamamoto, Y.Uesugi, Y.Kishimoto, H.kimura, M.Nagami, K.Itoh, S.I.Itoh and Y.Shimomura for many useful discussions. The authors would like to acknowledge Drs. S.Mori, K.Tomabechi and M.Yoshikawa for their continuous encouragement.

## 4. Summary

The FWCD is examined for a reactor grade tokamak plasma by using the ray tracing code and the quasi-linear Fokker-Planck code. When the wave frequency is selected to $f/f_{ci}>7$ with an appropriate wave spectrum, the ion cyclotron damping can be neglected and the normalized current drive efficiency $\eta_{CD}=\bar{n}_e(10^{19}\mathrm{m}^{-3})I_{RF}(\mathrm{A})R(\mathrm{m})/P_{RF}(\mathrm{W})\sim3.0$ can be expected in a high density ($\bar{n}_e=7\times10^{19}\mathrm{m}^{-3}$) and high temperature ($T_e$=40keV) plasma. The FWCD has the capability to control the current profile even in the reactor grade high temperature plasma.

The electron damping rate for the fast wave is weak even in high temperature plasma, for example, $P_{abs}/P_{in}\sim0.6$ at $T_e$=40keV. The RF power which is not absorbed in single path propagation also contribute to drive RF current. We have to introduce the multiple-path effect[9] in order to more precise efficiency and RF current profile.

## Acknowledgements

The authors are grateful to Drs. T.Yamamoto, Y.Uesugi, Y.Kishimoto, H.kimura, M.Nagami, K.Itoh, S.I.Itoh and Y.Shimomura for many useful discussions. The authors would like to acknowledge Drs. S.Mori, K.Tomabechi and M.Yoshikawa for their continuous encouragement.

REFERENCES

1. JT-60 Team, presented by R.Yoshino, Proc. 14th Europ. Conf. on Controlled Fusion and Plasma Phys., Madrid (1987).
2. K.Ushigusa, T.Imai, R.Yoshino et al., JAERI-M 87-012(1987).
3. T.Yamamoto and JFT-2 group, in Non-Inductive Current Drive in Tokamaks (Proc. IAEA Tech. Committee Meeting, Culham,1983), vol.1, (1983)224.
4. M.Porkolab, J.J.Schuss, B.Lloyd, et al., Phys. Rev. letters 53(1984)450.
5. K.Miyamoto, S.Sugihara, H.Kimura et al., JAERI-M 87-172(1987).
6. T.Yamamoto, Y.Uesugi, K.Hoshino et al.,JAERI-M 86-115(1986).
7. Y.Kishimoto, K.Hamamatsu, A.Fukuyama et al., Nuclear Fusion 27(1987)549.
8. J.G.Cordey, Plasma Phys. and Controlled Nuclear Fusion, 26(1984)123.
9. P.T.Bonoli and R.C.Englade, Phys. Fluids 29(1986)2937.

Table 1 Typical plasma parameters

| | |
|---|---|
| Major Radius $R_o$ ( m ) | 4.9 |
| Minor Radius $a_p$ ( m ) | 1.15 |
| Plasma Current $I_p$ ( MA ) | 8.0 |
| Toroidal Field $B_T$ ( T ) | 5.5 |
| Parameter Profile | Parabolic |
| Line density $\bar{n}_e$ ( $10^{19}m^{-3}$ ) | 7.0 |
| Temperature $T_e(0)=T_i(0)$ ( keV ) | 30 |
| Frequency $f$ ( GHz ) | 0.4 |
| $Z_{eff}$ | 1.5 |
| Gas | D |
| $n_{\parallel}(0)$ | 1.5 |
| $\Delta n_{\parallel}$ | 1.0 |

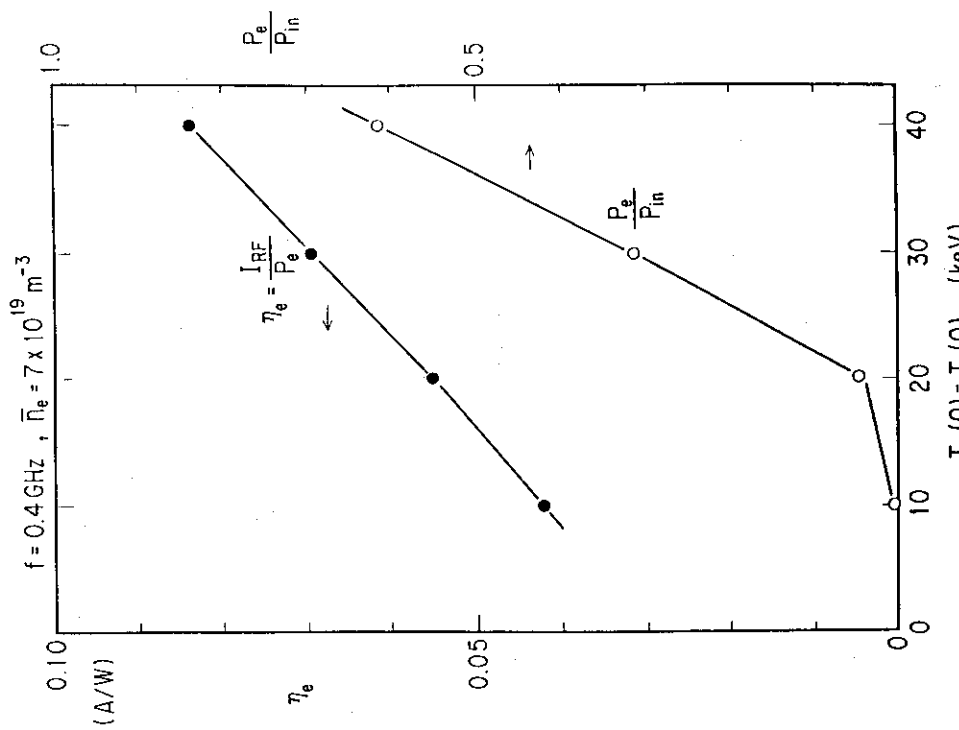


Fig. 2 Central temperature $T_e(0)=T_i(0)$ versus $\eta_e=I_{RF}/P_e$, $P_e/P_{in}$. f=0.4GHz, $\bar{n}_e=7\times10^{19}$ $m^{-3}$.

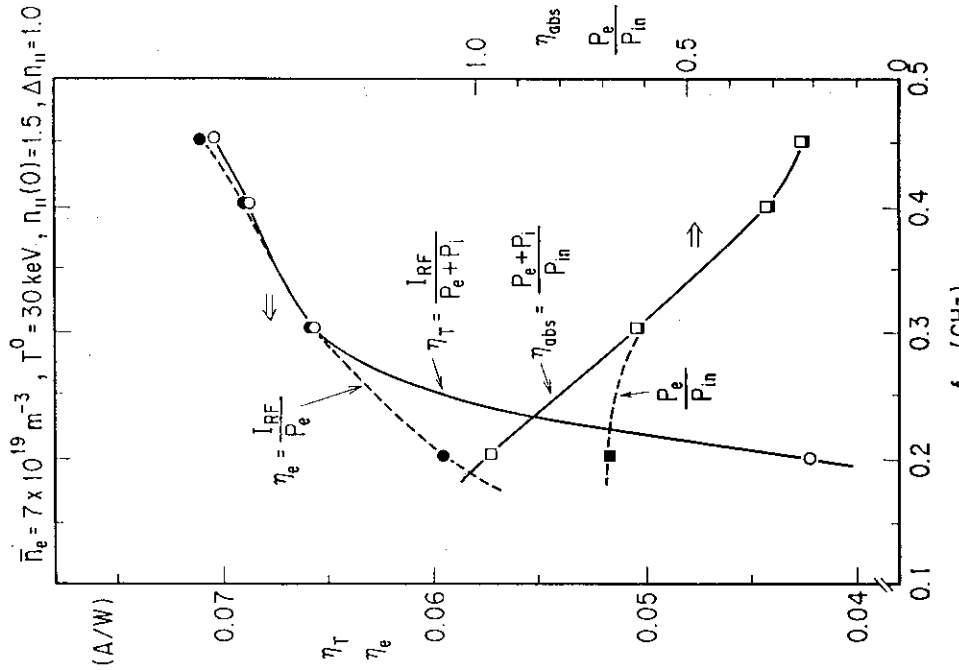


Fig. 1 Frequency dependence of $\eta_e=I_{RF}/P_e$, $\eta_T=I_{RF}/P_{abs}$, $\eta_{abs}=(P_e+P_i)/P_{in}$ and $P_e/P_{in}$. $\bar{n}_e=7\times10^{19}m^{-3}$, $T_e(0)=T_i(0)=30$keV.

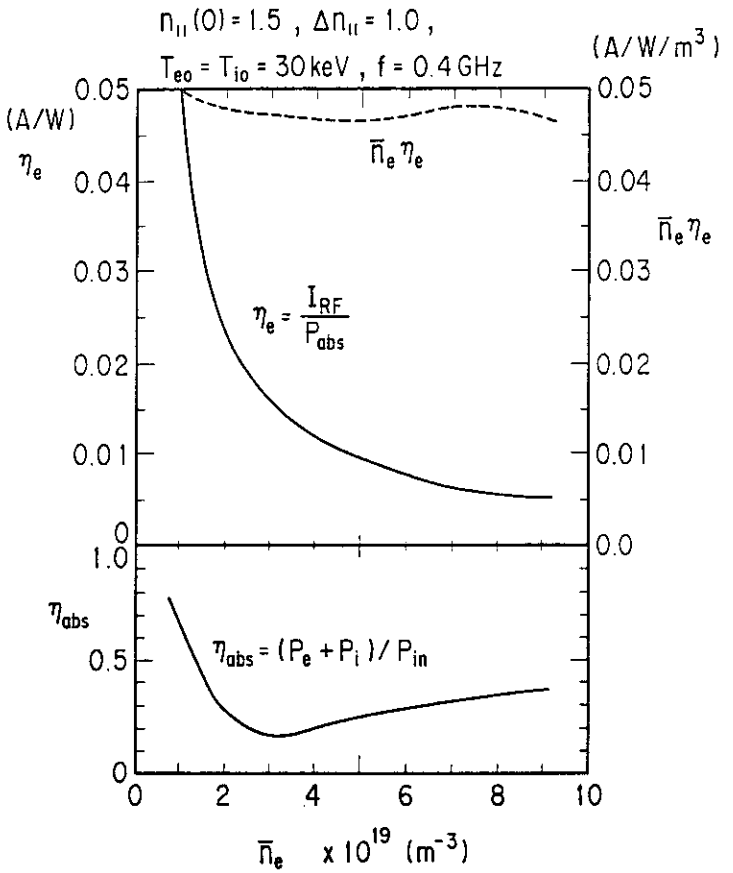


Fig. 3 Density dependence of $\eta_e = I_{RF}/P_e$, $\bar{\eta}_T = I_{RF}/P_{abs}$, $\bar{n}_e$ $I_{RF}/P_{abs}$, $P_{abs}/P_{in}$ f=0.4GHz, $T_e(0) = T_i(0) = 30$keV.

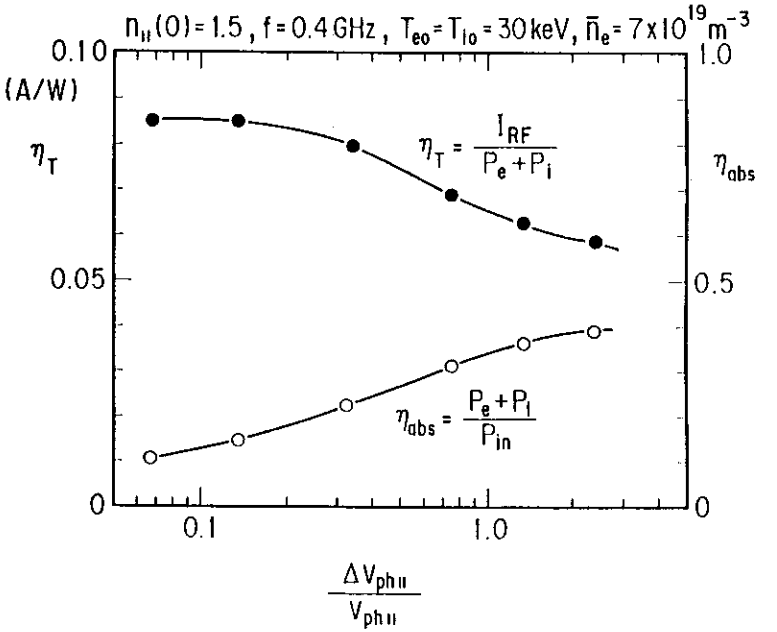


Fig. 4 $\eta_T = I_{RF}/P_{abs}$ and $\eta_{abs} = P_{abs}/P_{in}$ against the width of launched wave phase velocity normalized by the mean phase velocity $\Delta v_{ph\parallel}/\langle v_{ph\parallel} \rangle$. $\langle n_{\parallel} \rangle = 1.5$, f=0.4GHz, $T_e(0) = T_i(0) = 30$keV, $\bar{n}_e = 7 \times 10^{19} m^{-3}$.

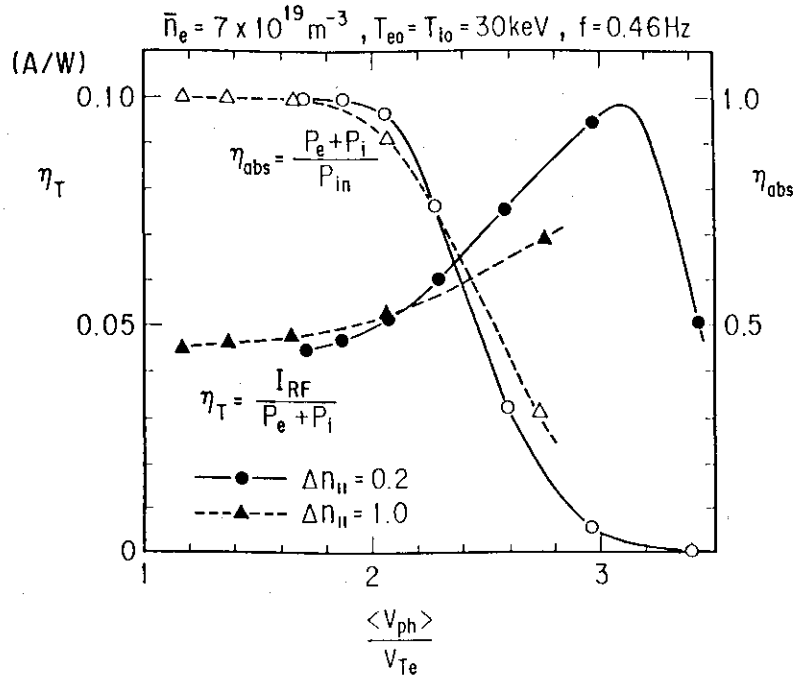


Fig. 5 $\eta_T = I_{RF}/P_{abs}$ and $\eta_{abs} = P_{abs}/P_{in}$ against the mean phase velocity normalized by the thermal velocity $\langle v_{ph\parallel} \rangle / v_e$. f=0.4GHz, $T_e(0) = T_i(0) = 30keV$, $\bar{n}_e = 7 \times 10^{19} m^{-3}$. Solid line is the case of $\Delta n_{\parallel} = 0.2$ and dotted line is $\Delta n_{\parallel} = 1.0$.

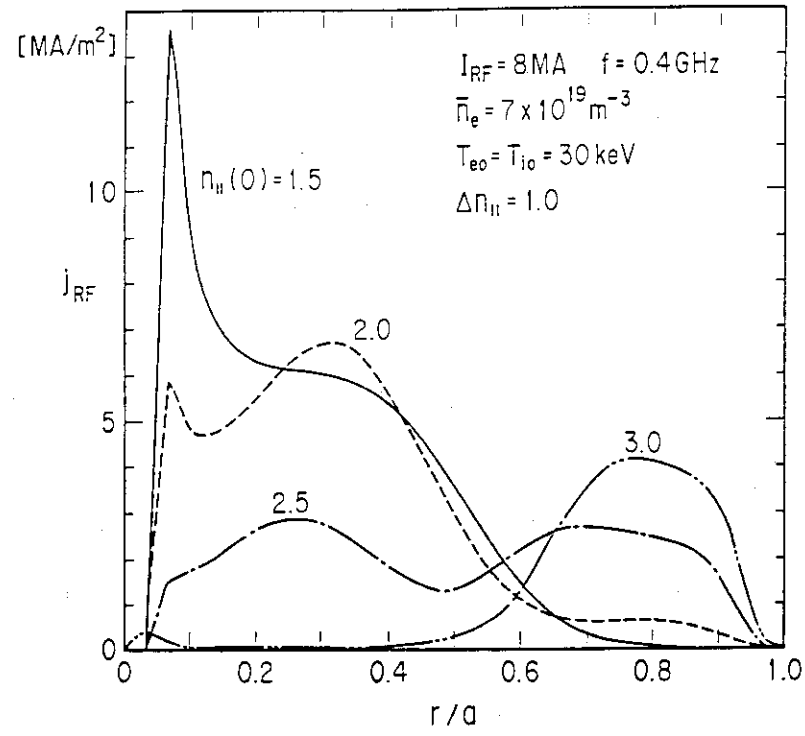


Fig. 6 The RF current profile for various $n_{\parallel}(0)$. f=0.4GHz, $T_e(0) = T_i(0) = 30keV$, $\bar{n}_e = 7 \times 10^{19} m^{-3}$ $\Delta n_{\parallel} = 1.0$

## Appendix

Numerical calculations of FWCD in JT-60 parameters (hydrogen plasma, $R_p$=3.15 m , $a_p$=0.85 m , $I_p$=2.0MA, $B_T$=4.0T, $T_e(0)=T_i(0)$=10keV) are shown in this appendix. In order to avoid the ion cyclotron damping, the wave frequency of $f$>0.6GHz($f/f_{ci}$>7) must be selected as mentioned in section 3. The comparison between the current drive efficiency of FWCD and LHCD is shown in Fig.A1, where $f$=0.9GHz with $n_{\parallel}$=0.5-2.3 for FWCD(solid line) and $f$=3.8GHz with $n_{\parallel}$=1.0-2.3 for LHCD(shadow region). At $\bar{n}_e>6\times10^{19}\mathrm{m}^{-3}$ the efficiency for FWCD is higher than that of LHCD. The degradation of efficiency for LHCD at high density comes from the accessibility condition of slow wave. The accessibility condition for a slow wave with 3.8GHz becomes $N_{\parallel}^{acc}$>1.6 in this condition. The FWCD is promising to drive RF current in a relatively high density plasma comparing with the LHCD. The normalized current drive efficiency for FWCD of $\eta_{CD}=\bar{n}_e(10^{19}\mathrm{m}^{-3})I_{RF}(\mathrm{A})R(\mathrm{m})/P_{RF}(\mathrm{W})$=1.1-2.0 can be expected in JT-60 parameters with 0.9GHz at $\bar{n}_e<10^{14}\mathrm{m}^{-3}$.

It is possible to test FWCD experimentally in JT-60 by using 0.12MHz ICRF heating system which can excite a travelling fast wave with $<n_{\parallel}>\sim3$ and $\Delta n_{\parallel}\sim8$ when the toroidal phasing of 2x2 loop antenna is set to be 90°. The RF current of 41kA can be numerically expected with the absorption power of about 1MW at $\bar{n}_e=2\times10^{19}\mathrm{m}^{-3}$, $B_T$=2.0T, $T_e(0)$=5keV and hydrogen plasma, which corresponds to $\eta_{CD}=\bar{n}_e I_{RF}R(\mathrm{m})/P_{RF}=0.24\times10^{19}\mathrm{m}^{-3}\mathrm{MA/MW}$. The efficiency is poor in this case because it is difficult to optimize the launched spectrum by the 2x2 loop antenna. However, when FW is applied to the LH heated or current driven plasma where high energy electrons up to several hundred keV exist, FW may enhance the RF current and high energy electrons. A principle proof of FWCD in a large tokamak may be demonstrated in such experiments.

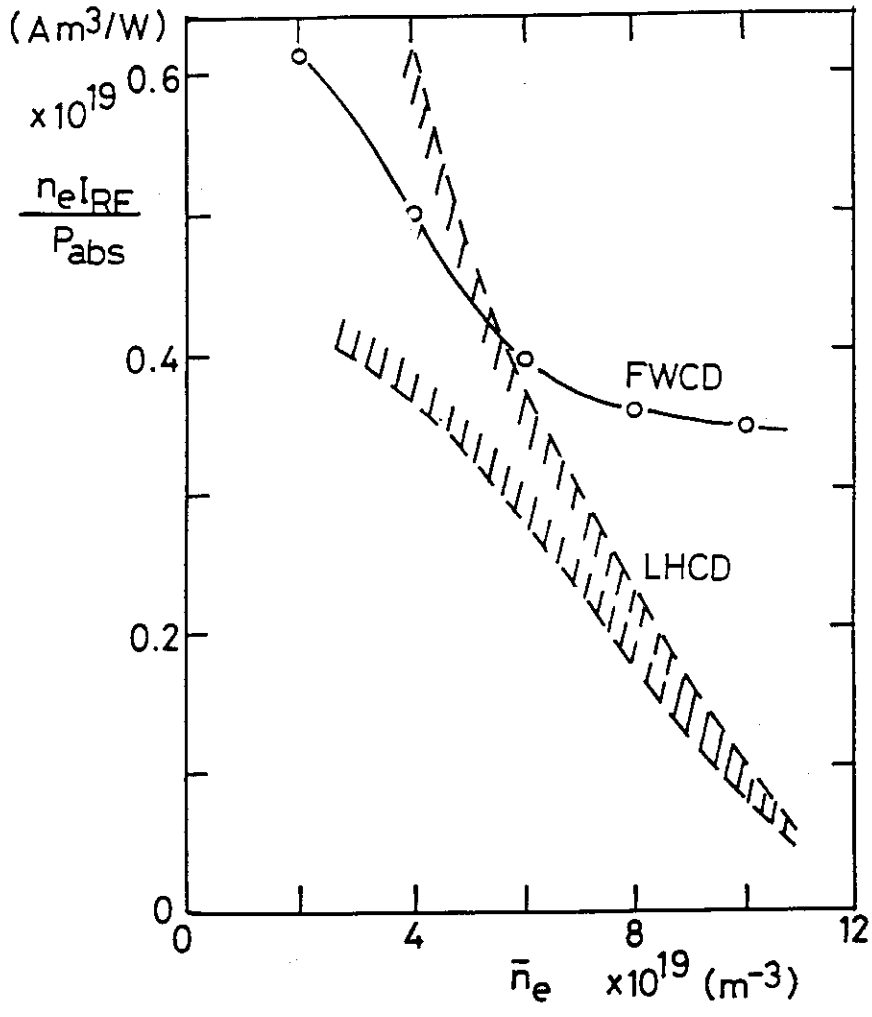


Fig. A1 Comparison of the density dependence of the current drive efficiency in JT-60 parameters for FWCD(0.9GHz, solid line) and LHCD(3.8GHz, shadow region) with the almost the same launched spectrum. Hydrogen plasma, $R_p$=3.15m, $a_p$=0.85m, $I_p$=2.0MA, $B_T$=4.0T, $T_e(0)=T_i(0)$= 10keV).